Human Molecular Genetics, 2013, Vol. 22, No. 23 **4698–4705**
doi:10.1093/hmg/ddt318
Advance Access published on July 11, 2013

Curcumin facilitates a transitory cellular stress response in *Trembler-J* mice

Yuji Okamoto[1], Davut Pehlivan[1], Wojciech Wiszniewski[1], Christine R. Beck[1], G. Jackson Snipes[2], James R. Lupski[1,3,4,*] and Mehrdad Khajavi[1,†]

[1]Department of Molecular and Human Genetics, [2]Department of Pathology and [3]Department of Pediatrics, Baylor College of Medicine, Houston, TX 77030, USA and [4]Texas Children's Hospital, Houston, TX 77030, USA

Received January 28, 2013; Revised June 4, 2013; Accepted July 1, 2013

We have previously shown that oral administration of curcumin significantly decreases the percentage of apoptotic Schwann cells and partially mitigates the severe neuropathy phenotype of the *Trembler-J* (*Tr-J*) mouse model in a dose-dependent manner. Here we compared the gene expression in sciatic nerves of 2-week-old pups and adult *Tr-J* with the same age groups of wild-type mice and found a significant increase in gene expression for hypoxia, inflammatory response and heat-shock proteins, the latter specifically the *Hsp70* family, in *Tr-J* mice. We also detected an activation of different branches of unfolded protein responses (UPRs) in *Tr-J* mice. Administering curcumin results in lower expression of UPR markers suggesting it relieves endoplasmic reticulum (ER) cell stress sensors in sciatic nerves of *Tr-J* mice while the level of heat-shock proteins stays comparable to untreated *Tr-J* mice. We further tested if *Hsp70* levels could influence the severity of the *Tr-J* neuropathy. Notably, reduced dosage of the *Hsp70* strongly potentiates the severity of the *Tr-J* neuropathy, though the absence of Hsp70 had little effect in wild-type mice. In aggregate, these data provide further insights into the pathological disease mechanisms caused by myelin gene mutations and further support the exploration of curcumin as a therapeutic approach for selected forms of inherited neuropathy and potentially for other genetic diseases due to ER-retained mutants.

INTRODUCTION

There have been tremendous advances in our understanding the molecular genetic bases of inherited peripheral neuropathies (1). This has revolutionized diagnostics, enabling an accurate and secure molecular diagnosis, precise recurrent risk estimates, prenatal diagnosis and better management of patients (2). However, there has been a partial failure to translate these findings into molecular based therapeutics. Currently, there is no effective small molecule or drug therapy for Charcot-Marie-Tooth (CMT) disease (3,4); supportive treatment is limited to rehabilitative therapy and surgical correction of skeletal deformities and soft-tissue abnormalities (5). Limited studies exist for treatments targeting different mutational mechanisms (Table 1).

Some myelin gene mutants (e.g. *MPZ* and *PMP22*) can cause severe disease (Dejerine-Sottas neuropathy, DSN; congenital hypomyelinating neuropathy, CHN) apparently by protein accumulation within the endoplasmic reticulum (ER), causing Schwann cell apoptosis, and subsequently peripheral neuropathy (6,7). Previous studies have shown that PMP22 is associated with ER chaperones during normal folding and such interactions are more prolonged with PMP22 mutants during quality control causing retention in the ER of Schwann cells (8–10). Accumulation of mutant PMP22 in the ER could be potentially accounted for by its interaction with calnexin (10) and perhaps triggering the unfolded protein response (UPR), resulting in Schwann cell death by apoptosis and subsequently, causing peripheral neuropathy (7,11). Previous studies in MpzS63del mice, a CMT1B mouse model, have shown that there is UPR activation in MPZS63del transgenic Schwann cells (12). Mutant MpzS63del is also retained in the ER, triggering the UPR as evidenced by significant changes in the UPR markers BiP [GRP78, a member of the heat-shock protein-70 (HSP70) family], CHOP and Downstream of CHOP genes (DOCs) (12). Although both MPZ and PMP22 are components of compact myelin and play major structural roles, MPZ accounts for more than 50% of the protein content of peripheral myelin (13); therefore, Schwann cells may be required to

*To whom correspondence should be addressed at: Department of Molecular and Human Genetics, Baylor College of Medicine, One Baylor Plaza, Room 604B, Houston, TX 77030, USA. Tel: +1 7137983723; Fax: +1 7137985073; Email: jlupski@bcm.edu
†Present address: Department of Vascular Biology, Boston Children's Hospital, Harvard Medical School, Boston, MA 02115, USA.

© *The Author 2013. Published by Oxford University Press. All rights reserved.*
For Permissions, please email: journals.permissions@oup.com

Table 1. Ongoing CMT studies based on novel therapeutic approaches [adapted from Fledrich *et al.*(37)]

Human disease	Mutation in patients	Clinical trial (for human)	Experimental therapy *in vivo*	Experimental therapy *in vitro*	Comment
CMT1A	*PMP22* duplication	Ascorbic acid	Ascorbic acid		None of the clinical trials reported beneficial effects of ascorbic acid to patients with CMT1A.
				P2X7 inhibition	
CMT1A/1E	*PMP22* point mutation	Neurotrophin-3 (for CMT1A)	Neurotrophin-3		Slight improvement of sensory and reflex scores but not of motor function. Number of patients' samples is small.
			Curcumin	Curcumin Rapamycin Geldanamycin	
			Caloric restriction		
CMT1B	*MPZ* point mutation		CHOP ablation		
			Curcumin Phosphatidylcoline curcumin derivative	Curcumin	
CMT2F/ HMN2B	*HPSB1; HSP27* point mutation		HDAC6 inhibition	HDAC6 inhibition	
CMTX	*Cx32/GJB1* point mutation		RAG-1 ablation		
			MCP-1 ablation CSF-1 ablation		
DSS/CHN	*PMP22* duplication	Ascorbic acid	Ascorbic acid		
				Rapamycin	

process higher levels of misfolded mutant MPZ compared with Tr-J mutant protein.

We previously demonstrated that curcumin, a small molecule compound derived from the curry spice tumeric, ameliorates the severity of the *Pmp22 Tr-J* neuropathy; an effect that correlates with decreased Schwann cell apoptosis (7). Curcumin has been reported to have anti-inflammatory and antitumor properties. Experiments in diverse disease animal models suggest that curcumin enables misfolded proteins to traverse from the ER to the plasma membrane concurrently reducing the cytotoxicity of the mutant protein (14–16). Although the exact mechanism by which curcumin corrects the processing of misfolded or aggregated mutant proteins in cells remains obscure, it appears that it modulates a number of cellular messenger/signaling pathways including NF-kB and intracellular calcium, interfering with the function of the ER calcium-dependent chaperones (15,17).

To elucidate the pathophysiology of the peripheral neuropathy disorder caused by *Tr-J* mutation, we investigated signal-transduction and stress pathways using focused gene expression arrays and compared gene expressions in sciatic nerves of 2-week-old pups and 4-month-old adult *Tr-J* with the same age groups of wild-type mice. Our data suggest that hypoxia induced, oxidative/metabolic stress, inflammatory response, heat-shock proteins, specifically the *Hsp70* family, and branches of UPRs are significantly increased in *Tr-J* mice. We then detected a decrease in the expression level of UPR components in curcumin-treated mice compared with untreated *Tr-J* mice suggesting that curcumin facilitates a transitory cellular ER stress response in *Tr-J* sciatic nerves. We also tested whether *Hsp70* levels could influence the severity of the *Tr-J* neuropathy. Remarkably, we found that *Tr-J* neuropathy was exacerbated by heterozygous or homozygous absence of *Hsp70*, whereas the absence of *Hsp70i* has no identifiable effect in wild- type mice.

RESULTS

Increase in heat-shock stress, apoptosis and inflammatory response signaling pathway genes in *Tr-J* sciatic nerves

From both human and mouse studies, it is clear that mutations affecting the *PMP22* gene cause demyelinating neuropathies; however, the normal biological functions of PMP22 and how mutants lead to disease remain poorly understood. Severely affected CMT1 patients with identical *PMP22* mutations and nerve biopsies show alterations analogous to those detected in heterozygous *Tr-J* mice (18). Thus, a better understanding of the pathophysiology of peripheral neuropathies caused by *Tr-J* could provide the basis for broadly applicable therapies. Here, we compared the patterns of gene expression in *Tr-J* and wild-type sciatic nerves of both 2-week-old pups and 4-month-old adult mice using stress and toxicity-specific pathway arrays. We identified 29 genes that are either up-regulated or down-regulated by *Tr-J* in pups and 28 genes in adult mice compared with wild-type mice (Table 2). The expressions of three groups of genes were significantly different: (i) apoptosis signaling genes such as *Fas*, *Casp1*; (ii) heat-shock proteins such as *Hspa4* (*Hsp70*) and (iii) inflammatory response genes such as *Cd40Ig*, *Ifng*, *Il1a*, *Il1b* and *Tnf*. These changes are in agreement with earlier findings of PMP22 mutant aggregation-induced apoptosis (7,11).

Pmp22 mutation causes ER stress in sciatic nerves

Previous studies have shown that both over-expression of wild-type *Pmp22* and mutant *Tr-J* protein form a complex with

calnexin, a Ca^{2+}-binding chaperone, that contributes to ER retention (10). Accumulation of *Pmp22* mutant *Tr-J* can also potentially trigger ER stress, resulting in Schwann cell death by apoptosis, and subsequently causing peripheral neuropathy (7,11). The mechanism by which the processing and function of misfolded or aggregated *Pmp22*, *Tr-J* mutant proteins in cells can be associated with apoptosis has not been determined. Nevertheless, it is hypothesized that it may include interference with the function of the ER chaperones. To determine the role of UPR in *Tr-J* mice, we analyzed different UPR markers including Bip, Chop, Atf3 and the oxidoreductase Ero1-lβ in sciatic nerves of both wild-type and *Tr-J* mice in two different age groups (2-week-old pups and 4-month-old adult mice, $n = 20$ in each group). We detected an increase of 1.34-, 1.54- and 1.29-fold of *BiP, Atf3* and *Ero1-lβ* mRNA levels in *Tr-J* pups and similarly 2.12-, 2.06-, 2.1- and 1.5-fold of *BiP, Atf3, Ero1-lβ* and Chop expression levels in *Tr-J* adults compared with wild-type pups and adults, respectively (Fig. 1A–D). We, however, did not detect significant increase in Chop mRNA expression levels in *Tr-J* pups (Fig. 1D, $P = 0.2$). We further verified and independently confirmed our findings by western analysis (Fig. 1E) in each group. In addition, we evaluated the possibility of *Tr-J* mutation inducing X-box binding protein (XBP-1) splicing in sciatic nerves. IRE-1, a serine/threonine protein kinase that possesses endonuclease activity, senses the accumulation of unfolded proteins in the lumen of the ER that leads to enzyme auto-activation (19). The active IRE-1 splices XBP-1 mRNA and converts it into a potent UPR transcriptional activator (19). We observed a high ratio of spliced XBP-1 in adult *Tr-J* mice (Fig. 1F) indicating a canonical UPR. Induction of multiple markers associated with activation of UPR leads to the up-regulation of certain ER chaperones and interference with folding of newly synthesized proteins suggesting a persistent ER stress that could be detrimental to cell growth and survival (20,21).

Table 2. Significant increases in hypoxia, heat shock, apoptosis and inflammatory response signaling genes in *Tr-J* sciatic nerves from both pups and adult mice.

Pathways	*Tr-J* pup	*Tr-J* adult
Apoptosis signaling	*Fas, Casp1*	*Fas, Tnfrsf1a*
Cell-cycle check point/ Arrest	*Hus1*	*Chek1, Chek2, Hus1, Rad51, Nbn*
Heat-shock proteins/ UPR	*Hspa41, Atf4, Ddit3, Dnajc3*	*Hspa41, Atf6b, Bid, Dnajc3*
Hypoxia	*Car9, Epo, Serpine, Slc2a1, Vegfa*	*Car9, Epo, Mmp9, Serpine, Vegfa*
Inflammatory response	*Cd40Ig, Crp, Ifng, Il1a, Il1b, Il6, Tnf*	*Cd40Ig, Crp, Ifng, Il1a, Il1b, Il6,*
Oxidative/Osmotic stress	*Fth1, Akr1b3, Aqp2, Aqp4, Cftr, Edn1, Nfat5*	*Txn1, Aqp2, Aqp4, Cftr, Edn1*

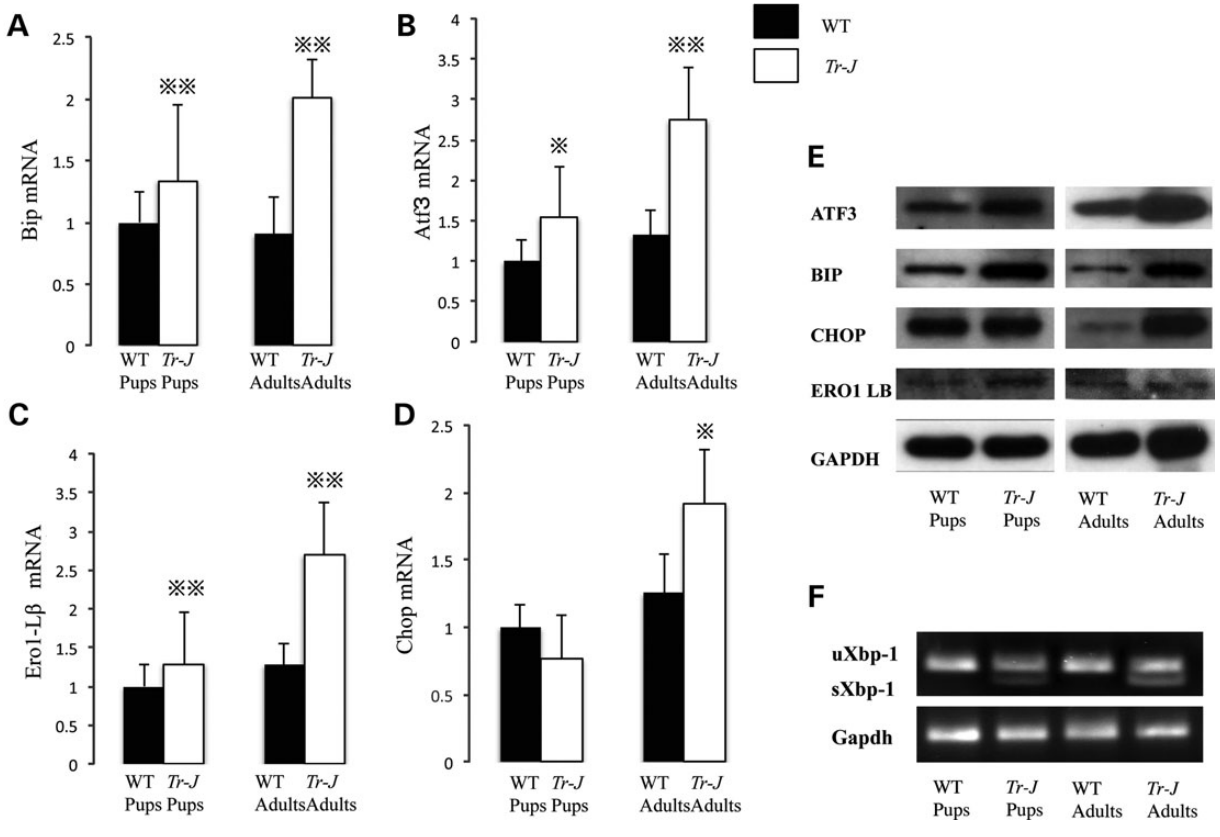

Figure 1. Activation of BiP (**A**), Atf3 (**B**), Ero1-lβ (**C**), Chop (**D**) in *Tr-J*. Expression levels in sciatic nerves were measured by quantitative RT–PCR using SYBR® Green in triplicates and normalized to β-Actin. All UPR markers except Chop in pups were significantly increased in 2-week-old pups and 4-month-old adult *Tr-J* compared with WT ($n = 20$ in Tr-J and WT). Error bars are standard error of the mean (SEM). (**E**) Western blot analysis of sciatic nerves was performed three times in two different sample groups. Our data shows an increase of UPR markers in both pups and adult *Tr-J* compared with WT, without CHOP expression levels in pups. (**F**) RT–PCR for XBP-1 unspliced (uXBP-1), spliced (sXBP-1) and Gapdh shows a high ratio of sXBP-1 in sciatic nerves of adult *Tr-J* mouse. $^{*}P < 0.05$ and $^{**}P < 0.005$.

Curcumin relieves ER stress in sciatic nerves of the *Tr-J* mouse

We previously showed that curcumin relieves the toxicity and/or cell stress associated with the *Tr-J* mutation and potentially enabling a more efficient protein-trafficking process in the ER that can result in increased axonal size and myelination that is sufficient to improve the clinical phenotype of *Tr-J* mice (7). Here, we analyzed the overall effect of curcumin on UPR components in sciatic nerves of curcumin-treated *Tr-J* mice. As shown in Figure 2, even though Bip and Chop mRNA levels were not reduced to wild-type level, the expression of UPR markers such as Atf3 and Ero1-lβ was decreased significantly to levels comparable with wild-type mice. We also measured the expression level of *Pmp22* in both curcumin-treated wild-type and *Tr-J* mice and found that *Pmp22* expression levels increased 1.4- and 1.5-fold in curcumin-treated wild-type and *Tr-J* mice, respectively (unpublished data). These findings support the contention that curcumin protects cells from ER stress-induced apoptosis by facilitating the cellular stress response yielding an overall reduction of stress, as evidenced by mitigation of marker gene expression, in *Tr-J* sciatic nerves.

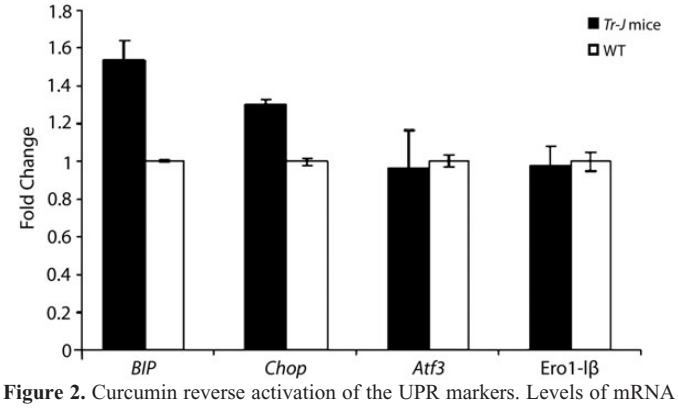

Figure 2. Curcumin reverse activation of the UPR markers. Levels of mRNA were measured by quantitative RT–PCR and normalized to 18S rRNA. BiP is still induced in curcumin-treated mice, whereas Chop, Atf3 and Ero1-lβ returned towards normal level after curcumin treatment. The age of the animals is 3-month-old adults.

Lack of *Hsp70* expression strongly potentiates the severity of the *Tr-J* neuropathy

Our gene expression analysis and previous immunocytochemical studies (22) suggest that heat-shock proteins, specifically Hsp70 and Hsp90, might be involved in the processing of impaired intracellular trafficking of mutant Pmp22. To test this directly, we crossed Hsp70i knockout mice (*Hsp70.1/3*$^{-/-}$) with *Tr-J* mice and evaluated the effects of reduced Hsp70i levels on the severity of the *Tr-J* neuropathy in adult animals using the rotarod test. As predicted, we found that the neuropathy in the *Tr-J* mice was severely aggravated by heterozygous or homozygous absence of Hsp70i, though the absence of Hsp70i had little effect on the rotarod performance of wild-type mice. In fact, double heterozygous mice (*Tr-J*$^{+/-}$/*Hsp70.1/3*$^{+/-}$) and *Hsp70i* null *Tr-J* (*Tr-J*$^{+/-}$/*Hsp70.1/3*$^{-/-}$) mice were unable to stay on the rotating rod, even at low angular velocity and after many trials (Fig. 3). This finding strongly suggests that reduced or absent Hsp70i may potentiate *Tr-J* mutation effects and that Hsp70 may directly be involved in intracellular processing of mutant Tr-J. We then sought to evaluate the effect of oral curcumin supplementation in mice with reduced *Hsp70* gene dosage. Unlike *Tr-J* mice, curcumin treatment did not improve the neuropathy of either *Tr-J*$^{+/-}$/*Hsp70.1/3*$^{+/-}$ or *Tr-J*$^{+/-}$/*Hsp70.1/3*$^{-/-}$. In fact, curcumin treatment was discontinued after 1 week because it had an apparent lethal side effect in this group of mice perhaps by potentiating the neuropathy. These findings suggest that curcumin may facilitate the stress response through potentiating the levels or function of HSP70.

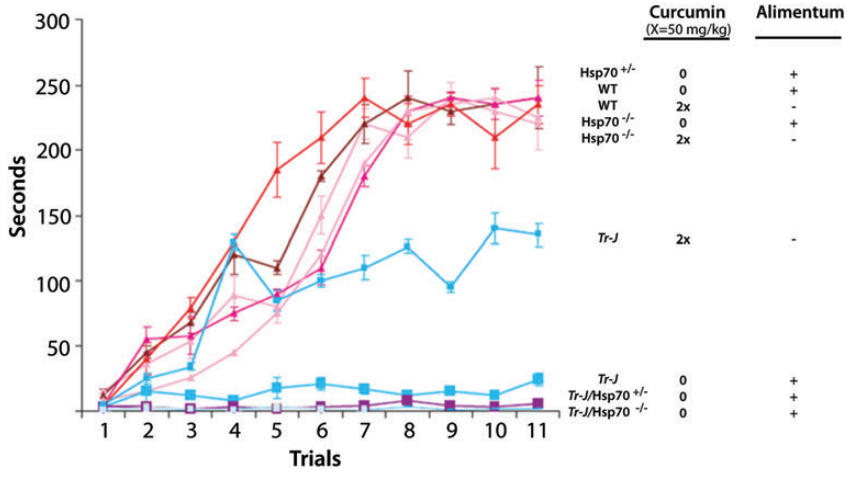

Figure 3. Neuromotor behavior in double heterozygous *Hsp70*/*Tr-J* and *Hsp70*$^{-/-}$/*Tr-J* mice. Rotarod test performed with 3-month-old wild-type (Wt), *Tr-J*, *Hsp70*$^{+/-}$/*Pmp22*$^{+/+}$ (*Hsp70*$^{+/-}$) *Hsp70*$^{-/-}$/*Pmp22*$^{+/+}$ (*Hsp70*$^{-/-}$), *Hsp70*$^{+/-}$/*Tr-J* and *Hsp70*$^{-/-}$/*Tr-J* and placebo-treated mice. In three series and 10 trials, the time that animals remained on a rod was measured and plotted. The rotation speed was increased every minute, from 16 to 36 rpm, in steps of 4 rpm. All animals were allowed to stay on the rod for a maximum of 270 s. The mean holding time of double heterozygous mice (*Tr-J*$^{+/-}$/*Hsp70.1/3*$^{+/-}$) and *Hsp70i* null *Tr-J* (*Tr-J*$^{+/-}$/*Hsp70.1/3*$^{-/-}$) mice was significantly lower than that of Wt and *Tr-J* ($P < 0.0001$ and $P < 0.01$).

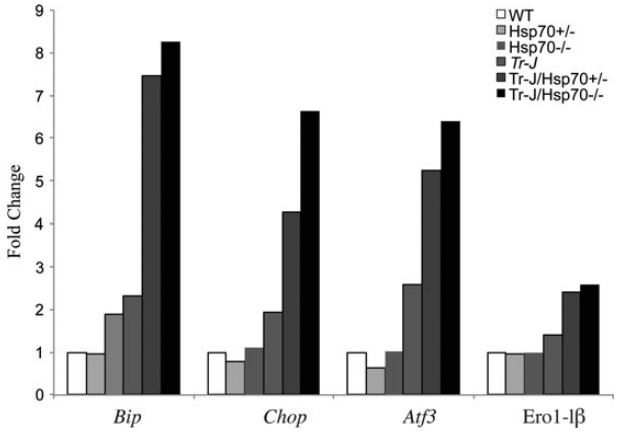

Figure 4. Activation of BiP and ER stress sensors-Chop, Atf3 and Ero1-lβin $Hsp70^{+/-}$/*Tr-J* and $Hsp70^{-/-}$/*Tr-J*. Expression levels in sciatic nerves were measured by quantitative RT–PCR and normalized to 18S rRNA. All UPR markers were significantly increased in $Hsp70^{+/-}$/*Tr-J* and $Hsp70^{-/-}$/*Tr-J* compared with wild-type (WT). There was no statistical difference in the expression levels of UPR between male and female mice.

UPR in low dosage of *Hsp70.1/3*

We analyzed different branches of UPR pathways in two different groups of mice: the first group was *Tr-J*$^{+/-}$/*Hsp70.1/3*$^{+/-}$ and *Tr-J*$^{+/-}$/*Hsp70.1/3*$^{-/-}$ and the second group included *Pmp22*$^{+/+}$/*Hsp70.1/3*$^{+/-}$ and *Pmp22*$^{+/+}$/*Hsp70.1/3*$^{-/-}$. We compared both groups with wild-type mice. As shown in Figure 4, *BiP* and *Chop* were increased 7.5- and 4.3-fold, respectively, in double heterozygous mice while an increase of 8.3- and 6.6-fold was observed in *Tr-J*$^{+/-}$/*Hsp70.1/3*$^{-/-}$ mice suggesting that UPR is activated as a protein quality control in this group. We also observed an increase of 5.3- and 2.4-fold in the expression of *Atf3* and *Ero1-lβ*, respectively, in double heterozygous mice while an increase of 6.4 and 2.6 of *Atf3* and *Ero1-lβ*, respectively, in *Hsp70i* null *Tr-J* mice (Fig. 4). Our data suggest an activation of UPR pathways in both double heterozygous and *Hsp70* null *Tr-J* mice as evidenced by significant increase in the expression of UPR markers; comparison between the groups suggest an *Hsp70* gene dosage-dependent effect. Notably, we did not observe any significant changes of UPR markers in *Pmp22*$^{+/+}$/*Hsp70*$^{+/-}$ and *Pmp22*$^{+/+}$/*Hsp70*$^{-/-}$ when compared with the wild-type.

DISCUSSION

We investigated specific molecular and cellular pathways through which curcumin may function to ameliorate the neuropathy in *Tr-J* mice and evaluated the effect of curcumin supplementation on the expression of genes associated with UPR pathways in sciatic nerves of *Tr-J* mice. We initially found that accumulation of Tr-J in the Schwann cell ER triggers UPR that leads to up-regulation of heat-shock proteins in *Tr-J* mice. The persistent ER stress activates apoptosis signaling genes such as *Caspase1* and *Fas* (TNF receptor superfamily member 6) consequently resulting in Schwann cell death by apoptosis. Recent studies have shown that ablation of Chop decreases demyelination in ER-stress-mediated neuropathy (12). We did not detect a significant increase ($P = 0.23$) in Chop levels between pups *Tr-J* and wild-type mice; however, adult *Tr-J* showed a significant increase in Chop compared with wild-type suggesting a potential time-dependent accumulation of stress. Similar to our results, Sancho *et al*. (11) showed that Schwann cell apoptosis occurs naturally in developing nerves of wild-type mice during the first postnatal 10 days and did not show significant differences between wild-type and *Tr* mice. However, at the age of 10 weeks, *Tr* mice showed a significant increase in Schwann cell density/proliferation and apoptosis at the same time.

There were a number of other markers such as Bip, Atf3 and Erol-1β that were significantly increased in sciatic nerves of both pup and adult *Tr-J* mice indicating the partial activation of UPR pathways. In fact, previous studies (12,23) have reported activation of UPR as the pathogenic mechanism for demyelination by misfolded Mpz mutants in different CMT1B mouse models. In a recent study of a more severe form of early onset CMT, a misfolded R98C Mpz mutant causes the activation of a 'canonical' UPR response (23). Interestingly, regular curcumin treatment showed a minor effect in improving neuropathy symptoms in the R98C CMT1B mouse model, whereas potentially more potent curcumin derivatives, dissolved in sesame oil or phophatidylcholine, rescue the motor deficit and ameliorated the neuropathy phenotype evidently by reducing the UPR activation (24). Mpz, however, is highly expressed in peripheral myelin and processing higher levels of misfolded mutant Mpz compared with Tr-J mutant proteins may potentially require a more potent treatment. We also observed a decrease in the expression level of UPR components in regular curcumin-treated mice compared with untreated *Tr-J* mice and did not detect any difference in the treatment outcome using curcumin dissolved in sesame oil in *Tr-J* mice (unpublished data).

There are a number of cellular mechanisms by which curcumin could act on *Tr-J* nerves; first, it is possible that curcumin might modulate signal-transduction pathways that regulate myelin gene expression. Alternatively, curcumin may act directly on neurons by acting on signal-transduction pathways, affecting the growth of myelinating Schwann cells potentially causing it to stimulate maturing axons to increase their caliber. Although this hypothesis may serve to explain the clinical effects of curcumin on the *Tr-J* neuropathy, it does not explain the reduced rate of apoptosis observed in curcumin-treated *Tr-J* sciatic nerves. Administering curcumin apparently results in the reduction of ER stress sensors in sciatic nerves of treated *Tr-J* mice. We have previously shown that curcumin treatment partially mitigates the clinical and neuropathological phenotype of *Tr-J* mice by relieving the toxic effect of the mutant PMP22, thereby inhibiting Schwann cell apoptosis and increasing axonal caliber and myelin thickness (7). The positive clinical response to curcumin occurs in a dose-dependent manner and is reversed after withdrawal of treatment. The ability of curcumin to increase axonal caliber and myelin thickness (7), without tomacula formation, is consistent with the hypothesis that curcumin relieves ER-associated degradation (ERAD) stress caused by abnormal processing of Pmp22 and/or other Schwann cell proteins that are required for myelination. We now show that this rescue is not due to reduced expression of the *Tr-J*, but due to reduced activation of the UPR. While the level of heat-shock proteins in curcumin-treated *Tr-J* stays comparable to untreated *Tr-J* mice, this could be expected in order to stabilize the

re-translocated mutant Pmp22 protein to the cytoplasm and potentially facilitate the Tr-J protein for subsequent degradation. Additionally, Patzko *et al*. (24) recently showed that curcumin decreases promyelinating transcription factors including c-Jun and SCIP (Oct6, Pou3f1) beside the UPR markers in heterozygous and homozygous R98C CMT1B mice. The heat-shock protein genes, specifically the Hsp70 family, showed the largest differences in our gene expression analyses of *Tr-J* nerves. The over-expression of heat-shock protein (*Hsp70*) has been shown to have a cytoprotective role against ischemia and other misfolding protein disorders such as spinal cerebellar ataxia 1 (25,26).

We further tested if *Hsp70* levels could influence the severity of the *Tr-J* neuropathy. Remarkably, we found that *Tr-J* neuropathy was severely affected by heterozygous or homozygous absence of *Hsp70*, even though the absence of *Hsp70* has no detectable effect in wild-type mice. Although morphological analysis could potentially provide additional insight into the worsening effect from lack of Hsp70 in sciatic nerves, our data provides evidence that this effect may be due to a general protective function of *Hsp70*, such as the one found in cancer cells fighting against cytotoxicity induced by anticancer agents that trigger the caspase-independent lysosomal cell-death pathway (27). Alternatively, Hsp70 may function as a necessary chaperone for Pmp22 prior to its degradation. In fact, in our curcumin treatment of $Tr\text{-}J^{+/-}/Hsp70.1/3^{+/-}$ mice, we found that the level of Hsp70 is critical after treatment with curcumin to process re-translocated Tr-J mutant in cytoplasm. In the absence of Hsp70, curcumin treatment had an apparent lethal side effect in $Tr\text{-}J^{+/-}/Hsp70.1/3^{+/-}$ mice presumably by potentiating the neuropathy. In this case, Hsp70 may help stabilize aggregation-prone regions of Pmp22, as it traverses the cytoplasm to the proteasome. It has been shown that Hsp70 chaperones function as facilitators for degradation either by preventing aggregation and/or actively transferring them to the proteolytic system (28). Other heat-shock proteins have been shown to play a role in different types of CMT disease such as mutations in the 27 kDa small heat-shock protein gene (*HSPB1*, also called *HSP27*) causing axonal CMT type 2F and distal hereditary motor neuropathy (distal HMN) (29). HSPB1 acts as a chaperone by binding misfolded or denatured proteins, and prevents them from forming toxic aggregates (30,31). Mutant HSPB1 decreases acetylated α-tubulin levels and decreases axonal transport. In addition, another study has shown that heat-shock protein 90 (HSP90) inhibitors enhance cytosolic chaperones, including HSP27 and HSP70, and improve myelination in neuropathic mouse cell lines (32).

Studies that increase expression of Hsp70 by using transgenic mouse models could potentially identify novel factors involved in glycoprotein ERAD of transmembrane folding defects. It is critical to understand the differences in how various myelin gene mutant proteins interact with the protein quality control machinery, because this could provide the basis for determining which chemical chaperone therapeutic strategies might be useful for specific protein-folding disorders. Rational drug design could be based on different principles, such as interfering with chaperone activity and allowing misfolded proteins to make their way out of the ER, or involving upregulation at the transcriptional level and modulation of protein-folding steps (33). Interestingly, one of the reported effects of curcumin is to induce the expression of *Hsp70* (28,34). This may partially explain the mechanism by which curcumin acts on Schwann cell apoptosis and ameliorates the *Tr-J* neuropathy (7). It also provides further evidence for the importance of ERAD pathways in the pathogenesis of CMT.

Together, these data provide insights into the pathological disease mechanisms caused by myelin gene mutations and identify new candidate genes that are likely to play important roles in disease process and may provide potential targets for therapeutic approaches to ER-retained mutants.

MATERIALS AND METHODS

Sample collection, RNA extraction and western blot analysis

Matings between *Tr-J* heterozygous females and males in the C57BL/6 genetic background were implemented to generate *Tr-J* heterozygous and wild-type controls. Tail DNAs were used for genotyping. We also crossed *Hsp70i* knockout mice ($Hsp70.1/3^{-/-}$) (35) with heterozygous *Tr-J* mice. These mice were obtained from a breeding colony of *Tr-J* and $Hsp70.1/3^{-/-}$ mice that we established in collaboration with G. Jackson Snipes, MD, PhD in our mouse facility. The sciatic nerves were dissected and frozen immediately in liquid nitrogen, and stored in −80°C. For RNA extraction, the sciatic nerves were homogenized in Trizol and RNA extracted according to the manufacturer's instruction (Invitrogen, Carlsbad, CA, USA) followed by purification on columns from RNeasy mini kit (Qiagen Sciences, Germantown, MD, USA). RNA quality was assessed using Agilent Bioanalyzer 2100 and the NanoDrop ND-1000 spectrophotometer. For western blot analysis, frozen sciatic nerves were pulverized, dissolved in lysis buffer containing 5 mM Tris−HCl (pH 7.5), 1.5 mM KCl, 2.5 mM $MgCl_2$, 1% deoxycholic acid, 1% Triton X-100, supplement with protease inhibitor cocktail (Roche, Indianapolis, IN, USA). The protein content of supernatant was determined using a BSA standard curve (BCA Protein Assay Kit, Thermo, Rockford, IL, USA). Equal amounts of the protein were electrophoresed on 12% SDS−polyacrylamide gels, and then transferred to PVDF membranes (Bio-Rad, Hercules, CA, USA). The blots were blocked for overnight at 4°C with 5% blotting-grade blocker (Bip-rad, Hercules, CA, USA) in TBS and then incubated with specific primary antibody, Gapdh (1:2000, MILLPORE, Temecula, CA, USA), Atf-3 (1:1000, Sigma, St Louis, MO, USA), Bip (1:2000, Sigma), Chop (1:2000 Thermo, Rockford, IL,USA) and Ero1-LB (1:200 Proteintech, Chicago, IL, USA) in PBST with 5% blotting-grade blocker. Following three washes with PBST, the blots were incubated with horseradish peroxidase (HRP)-conjugated secondary antibodies (1:1000−1:10000 dilution; Bio-rad). After three washes with PBST, the transferred proteins were detected using chemiluminescent (ECL) substrate for HRP (Supersignal West Pico Chemiluminescent Substrate, Thermo) with X-ray film.

Microarray processing and quantitative RT−PCR

Five to 10 μg of total RNA from each individual sciatic nerves of 4 *Tr-J* at 2 weeks and 4 months of age and four wild-type controls were used to produce cDNA target for microarray. The target was generated using a reverse transcription reaction to produce

cDNA (Supercript Choice System, Invitrogen, Carlsbad, CA, USA). For PCR array data (Qiagen Sciences, Germantown, MD, USA) analysis, the ΔΔCt method was used and each gene fold-change was calculated as difference in gene expression between *Tr-J* and wild-type samples. Data were normalized against two housekeeping genes that were included in the PCR array by subtracting the average Ct value for two housekeeping genes from the average Ct value of gene of interest. ΔΔCt were compared across groups using *t*-tests. The *P*-value is calculated based on whether the test sample score is from the extreme case of scores from control treatment samples with compound not causing the toxic effect under evaluation (Qiagen Sciences, Germantown, MD, USA). The *P*-value is considered significant when it is <0.05. To verify changes in the expression level of specific genes identified on the microarray, additional real-time RT–PCR analyses was performed. Total RNA of 2 μg for each sample was reverse transcribed with the Superscript First-strand cDNA synthesis kit (Invitrogen, Carlsbad, CA, USA) using a random primer. The cDNA was then PCR-amplified in triplicates and confirmed in two independent experiments by SYBR® Green PCR Master Mix (Applied Biosystems, Foster City, CA, USA) using 7900HT Fast Real-Time PCR System (Applied Biosystems, Foster City, CA, USA) on different animal groups to avoid biases. The primers were designed by using Universal Library Assay Design Center of Roche Applied Science web site (https://www.roche-applied-science.com/sis/rtpcr/upl/index.jsp?id=UP030000) (Roche Diagnostics Corporation Roche Applied Science, Indianapolis, USA) and RT Primer database (http://medgen.ugent.be/rtprimerdb/). For XBP-1, RT–PCR was performed as described previously (36). The relative level of each RNA sample is calculated using the ΔΔCt method normalized either to the corresponding Gapdh or β-Actin levels.

Curcumin treatment and specific motor response tests (motor activity on a rotating rod)

Curcumin treatment was performed as described previously (7). The animals' locomotor performances were tested using a rotarod test, a motor co-ordination and balance control task. Briefly, in every test, the exams were masked to the specific genotype. Each mouse underwent the same 5-day procedure. The first 2 days were used to train the animals [five sessions of 2 min walking were run at a very low speed, i.e. 5 rotations per minute (rpm)] until a steady baseline level was reached in their performances. The mice were then subjected to a higher rotation speed to familiarize them with the forthcoming experimental conditions. The last 3 days were used to run the test sessions. Here the mice had to perform two series of five trials with a 1 h rest period between the two series. In each trial, the mouse was placed on the rod and the rotation speed was increased every minute from 16 to 36 rpm in steps of 4 rpm. The scores obtained in this test were measured based on the time spent on the rod without falling minus the time during which the mouse is rotating with the rod without falling (7). The mean walking time spent on the rod was then calculated for each genotype at each rotation speed. As this task is very demanding for the mice, we will make sure the results are not affected by fatigue. Each individual's performances were compared between the first and last trials at the maximum speed (paired *t*-test).

Conflict of Interest statement. J.R.L. is a paid consultant for Athena Diagnostics, has stock ownership in 23andMe and Ion Torrent Systems and is a co-inventor on multiple United States and European patents related to molecular diagnostics for inherited neuropathies, eye diseases and bacterial genomic fingerprinting. The Department of Molecular and Human Genetics at Baylor College of Medicine derives revenue from the chromosomal microarray analysis offered in the Medical Genetics Laboratory.

FUNDING

This work was supported in part by US National Institute of Neurological Disorders and Stroke, National Institutes of Health (NINDS, NIH) grant (R01NS058529). W.W. is supported by a (K23NS078056) grant from the NINDS, NIH.

REFERENCES

1. Szigeti, K. and Lupski, J.R. (2007) Hereditary motor and sensory neuropathies. In Rimoin, D.L., Connor, J.M., Pyeritz, R.E. and Korf, BR (eds), *Emory and Rimoin's Principles and Practice of Medical Genetics*. Churchill Livingstone Elsevier, Philadelphia, pp. 2946–2962.
2. Szigeti, K. and Lupski, J.R. (2009) Charcot-Marie-Tooth disease. *Eur. J. Hum. Genet.*, **17**, 703–710.
3. Young, P., De Jonghe, P., Stogbauer, F. and Butterfass-Bahloul, T. (2008) Treatment for Charcot-Marie-Tooth disease. *Cochrane Database Syst. Rev.*, CD006052.
4. Reilly, M.M., Shy, M.E., Muntoni, F. and Pareyson, D. (2010) 168th ENMC International Workshop: outcome measures and clinical trials in Charcot-Marie-Tooth disease (CMT). *Neuromuscul. Disord.*, **20**, 839–846.
5. Pareyson, D. and Marchesi, C. (2009) Natural history and treatment of peripheral inherited neuropathies. *Adv. Exp. Med. Biol.*, **652**, 207–224.
6. Khajavi, M., Inoue, K., Wiszniewski, W., Ohyama, T., Snipes, G.J. and Lupski, J.R. (2005) Curcumin treatment abrogates endoplasmic reticulum retention and aggregation-induced apoptosis associated with neuropathy-causing myelin protein zero-truncating mutants. *Am. J. Hum. Genet.*, **77**, 841–850.
7. Khajavi, M., Shiga, K., Wiszniewski, W., He, F., Shaw, C.A., Yan, J., Wensel, T.G., Snipes, G.J. and Lupski, J.R. (2007) Oral curcumin mitigates the clinical and neuropathologic phenotype of the Trembler-J mouse: a potential therapy for inherited neuropathy. *Am. J. Hum. Genet.*, **81**, 438–453.
8. Colby, J., Nicholson, R., Dickson, K.M., Orfali, W., Naef, R., Suter, U. and Snipes, G.J. (2000) PMP22 carrying the trembler or trembler-J mutation is intracellularly retained in myelinating Schwann cells. *Neurobiol. Dis.*, **7**, 561–573.
9. Fortun, J., Go, J.C., Li, J., Amici, S.A., Dunn, W.A. Jr. and Notterpek, L. (2006) Alterations in degradative pathways and protein aggregation in a neuropathy model based on PMP22 overexpression. *Neurobiol. Dis.*, **22**, 153–164.
10. Dickson, K.M., Bergeron, J.J., Shames, I., Colby, J., Nguyen, D.T., Chevet, E., Thomas, D.Y. and Snipes, G.J. (2002) Association of calnexin with mutant peripheral myelin protein-22 ex vivo: a basis for 'gain-of-function' ER diseases. *Proc. Natl Acad. Sci. USA*, **99**, 9852–9857.
11. Sancho, S., Young, P. and Suter, U. (2001) Regulation of Schwann cell proliferation and apoptosis in PMP22-deficient mice and mouse models of Charcot-Marie-Tooth disease type 1A. *Brain*, **124**, 2177–2187.
12. Pennuto, M., Tinelli, E., Malaguti, M., Del Carro, U., D'Antonio, M., Ron, D., Quattrini, A., Feltri, M.L. and Wrabetz, L. (2008) Ablation of the UPR-mediator CHOP restores motor function and reduces demyelination in Charcot-Marie-Tooth 1B mice. *Neuron*, **57**, 393–405.
13. Niemann, A., Berger, P. and Suter, U. (2006) Pathomechanisms of mutant proteins in Charcot-Marie-Tooth disease. *Neuromol. Med.*, **8**, 217–242.
14. Vasireddy, V., Chavali, V.R., Joseph, V.T., Kadam, R., Lin, J.H., Jamison, J.A., Kompella, U.B., Reddy, G.B. and Ayyagari, R. (2011) Rescue of photoreceptor degeneration by curcumin in transgenic rats with P23H rhodopsin mutation. *PLoS One*, **6**, e21193.

15. Egan, M.E., Pearson, M., Weiner, S.A., Rajendran, V., Rubin, D., Glockner-Pagel, J., Canny, S., Du, K., Lukacs, G.L. and Caplan, M.J. (2004) Curcumin, a major constituent of turmeric, corrects cystic fibrosis defects. *Science*, **304**, 600–602.
16. Wang, Y., Xiao, J., Zhou, H., Yang, S., Wu, X., Jiang, C., Zhao, Y., Liang, D., Li, X. and Liang, G. (2011) A novel monocarbonyl analogue of curcumin, (1E,4E)-1,5-bis(2,3-dimethoxyphenyl)penta-1,4-dien-3-one, induced cancer cell H460 apoptosis via activation of endoplasmic reticulum stress signaling pathway. *J. Med. Chem.*, **54**, 3768–3778.
17. Acosta, D., Affolder, T., Akimoto, H., Albrow, M.G., Ambrose, D., Amidei, D., Anikeev, K., Antos, J., Apollinari, G., Arisawa, T. *et al.* (2004) Search for pair production of scalar top quarks in R-parity violating decay modes in pp collisions at square root of s = 1.8 TeV. *Phys. Rev. Lett.*, **92**, 051803.
18. Martini, R. (1997) Animal models for inherited peripheral neuropathies. *J. Anat.*, **191**, 321–336.
19. Yoshida, H., Matsui, T., Yamamoto, A., Okada, T. and Mori, K. (2001) XBP1 mRNA is induced by ATF6 and spliced by IRE1 in response to ER stress to produce a highly active transcription factor. *Cell*, **107**, 881–891.
20. Gething, M.J. (1999) Role and regulation of the ER chaperone BiP. *Semin. Cell Dev. Biol.*, **10**, 465–472.
21. Zinszner, H., Kuroda, M., Wang, X., Batchvarova, N., Lightfoot, R.T., Remotti, H., Stevens, J.L. and Ron, D. (1998) CHOP is implicated in programmed cell death in response to impaired function of the endoplasmic reticulum. *Genes Dev.*, **12**, 982–995.
22. Ryan, M.C., Shooter, E.M. and Notterpek, L. (2002) Aggresome formation in neuropathy models based on peripheral myelin protein 22 mutations. *Neurobiol. Dis.*, **10**, 109–118.
23. Saporta, M.A., Shy, B.R., Patzko, A., Bai, Y., Pennuto, M., Ferri, C., Tinelli, E., Saveri, P., Kirschner, D., Crowther, M. *et al.* (2012) Mpzr98c arrests Schwann cell development in a mouse model of early-onset Charcot-Marie-Tooth disease type 1B. *Brain*, **135**, 2032–2047.
24. Patzko, A., Bai, Y., Saporta, M.A., Katona, I., Wu, X., Vizzuso, D., Feltri, M.L., Wang, S., Dillon, L.M., Kamholz, J. *et al.* (2012) Curcumin derivatives promote Schwann cell differentiation and improve neuropathy in R98C CMT1B mice. *Brain*, **135**, 3551–3566.
25. Cummings, C.J., Sun, Y., Opal, P., Antalffy, B., Mestril, R., Orr, H.T., Dillmann, W.H. and Zoghbi, H.Y. (2001) Over-expression of inducible HSP70 chaperone suppresses neuropathology and improves motor function in SCA1 mice. *Hum. Mol. Genet.*, **10**, 1511–1518.
26. Noble, E.G., Milne, K.J. and Melling, C.W. (2008) Heat shock proteins and exercise: a primer. *Appl. Physiol. Nutr. Metab.*, **33**, 1050–1065.
27. Daugaard, M., Kirkegaard-Sorensen, T., Ostenfeld, M.S., Aaboe, M., Hoyer-Hansen, M., Orntoft, T.F., Rohde, M. and Jaattela, M. (2007) Lens epithelium-derived growth factor is an Hsp70–2 regulated guardian of lysosomal stability in human cancer. *Cancer Res.*, **67**, 2559–2567.
28. Morton, J.P., Kayani, A.C., McArdle, A. and Drust, B. (2009) The exercise-induced stress response of skeletal muscle, with specific emphasis on humans. *Sports Med.*, **39**, 643–662.
29. Evgrafov, O.V., Mersiyanova, I., Irobi, J., Van Den Bosch, L., Dierick, I., Leung, C.L., Schagina, O., Verpoorten, N., Van Impe, K., Fedotov, V. *et al.* (2004) Mutant small heat-shock protein 27 causes axonal Charcot-Marie-Tooth disease and distal hereditary motor neuropathy. *Nat. Genet.*, **36**, 602–606.
30. Arrigo, A.P. (2007) The cellular 'networking' of mammalian Hsp27 and its functions in the control of protein folding, redox state and apoptosis. *Adv. Exp. Med. Biol.*, **594**, 14–26.
31. Dierick, I., Irobi, J., De Jonghe, P. and Timmerman, V. (2005) Small heat shock proteins in inherited peripheral neuropathies. *Ann. Med.*, **37**, 413–422.
32. Rangaraju, S., Madorsky, I., Pileggi, J.G., Kamal, A. and Notterpek, L. (2008) Pharmacological induction of the heat shock response improves myelination in a neuropathic model. *Neurobiol. Dis.*, **32**, 105–115.
33. Khajavi, M. and Lupski, J.R. (2008) Balancing between adaptive and maladaptive cellular stress responses in peripheral neuropathy. *Neuron*, **57**, 329–330.
34. Silver, J.T. and Noble, E.G. (2012) Regulation of survival gene hsp70. *Cell Stress Chaperones*, **17**, 1–9.
35. Hunt, C.R., Dix, D.J., Sharma, G.G., Pandita, R.K., Gupta, A., Funk, M. and Pandita, T.K. (2004) Genomic instability and enhanced radiosensitivity in Hsp70.1- and Hsp70.3-deficient mice. *Mol. Cell Biol.*, **24**, 899–911.
36. Samali, A., Fitzgerald, U., Deegan, S. and Gupta, S. (2010) Methods for monitoring endoplasmic reticulum stress and the unfolded protein response. *Int. J. Cell. Biol.*, **2010**, 830307.
37. Fledrich, R., Stassart, R.M. and Sereda, M.W. (2012) Murine therapeutic models for Charcot-Marie-Tooth (CMT) disease. *Br. Med. Bull.*, **102**, 89–113.